Proceeding of the IEEE
International Conference on Robotics and Biomimetics
Dali, China, December 2019

Simulation for Multi-point Haptic Feedback Based on Ultrasound Phased Array

Yuyang Yuan
Department of Mechatronics
Harbin Institute of Technology
Shenzhen, China
hiruruku@outlook.com

Zhili Long
Department of Mechatronics
Harbin Institute of Technology
Shenzhen, China
Corresponding author:
longzhili@hit.edu.cn

Zhaotian Jiang
Department of Mechatronics
Harbin Institute of Technology
Shenzhen, China
Jiangzt111@outlook.com

Cong Li
Department of Mechatronics
Harbin Institute of Technology
Shenzhen, China
731342693@qq.com

***Abstract*—As a new type of interaction way, haptic feedback has attracted a lot of attention. Among different kinds of haptic feedback methods, contactless haptic feedback based on ultrasound array has become one of the most promising methods because of its simple structure, low cost, diverse feedback forms and flexible adjustment. This paper firstly discusses the mechanism of human body's tactile sensation in detail, and then analyzes the mechanism of the realization of haptic feedback by ultrasound phased array. Then the mathematical model of ultrasound phased array's acoustic field is established, and the methods for solving single point and multi-point haptic feedback are presented. The energy efficiency is further optimized for the solution of multi-point haptic feedback.**

Keywords—ultrasound phased array; tactile sensation mechanism; multi-point haptic feedback ; acoustic field optimization

I. INTRODUCTION

With the development of virtual reality technology, the demand for better human-computer interaction process is also growing. Haptic feedback technology is one of the frontier areas with both great challenge and expectations. Compared with sight, hearing and taste, the sense of touch often get less attention. However, it plays a vital role in daily life. A study of Microsoft in 2015 showed that when typing on a touch screen with vibrotactile feedback, typing speed is faster and error rate is lower[1].

Early tactile feedback methods mainly utilized the skin's response to stimulations of vibration, local shape or pressure distribution, temperature and so on. In 1993, Salisbury et al. from the MIT Artificial Intelligence Laboratory developed a haptic force feedback device called PHANToM[2]. The user feels the force feedback through the resistance transmitted by its operating end, which has 6 degrees of freedom. In addition, there are also a variety of data gloves used in VR games in recent years [3]. Although these devices have the advantages of large feedback force, high control precision or high positional accuracy, they are more likely to be complicated in structure, bulky, expensive, or have limited operating space.

Several contactless haptic feedback methods are then be proposed. In 2005, Suzuki Yuriko et al. designed a gas injection force/haptic feedback system using air pressure[4]. The operator's finger position is obtained by camera, and then the nozzle is controlled to inject gas at the corresponding position, eventually generating pressure at the finger. In 2013, Gupta et al. designed a system called AirWave which utilizes gas vortex ring[5]. The tactile sensation is generated by a box-shaped gas vortex ring generator. When the air inside the box is pushed outward through the ring, it is rapidly rotated by the compression, and finally ejected in the form of an air ring, eventually forming tactile sensation. Similar system like AIREAL was proposed by Rajinder et al. in the same year[6]. However, airflow is messy and the duration is short. Besides, their spray direction is fixed and the generated pressure is relatively small. In 2011, Weiss et al. designed the FingerFlux system based on electromagnet array[7]. Its disadvantage is that the operator needs to stick the permanent magnet on the finger and the effective distance range is small.

In 2008, Shinoda et al. proposed the idea of generating non-contact haptic feedback over the air directly based on the form of ultrasound array focusing, and designed their first ultrasound array prototype[8]. They've made great effort to further explore the potential of ultrasound array and many interesting interactive systems such as Haptomime were designed[9]. These interactive systems, combining visual and tactile sensations properly, enable operators to have a better interactive experience. In addition, the haptic feedback system Ultrahaptics designed by Tom Carter et.al from the University of Bristol realized haptic feedback of multiple points and can even form volumetric shapes[10-11]. The haptic feedback method based on ultrasound phased array controls energy distribution of the acoustic field to generate focused point with high energy density, eventually stimulating human receptors. The whole process does not need any contact with the operator. Although the feedback force is small, but its control is flexible, the feedback form is diverse, and the overall cost is relatively low, which shows great potential of ultrasound arrays.

In this paper, the mechanism of haptic feedback generated by ultrasound phased array is introduced. Then the acoustic field of ultrasound phased array is modeled and simulated. Based on its mathematical model, this paper analyzes and deduces the solution of single and multi-point haptic feedback. Moreover, solution for multi-point haptic feedback is further optimized to achieve higher power efficiency.

II. METHODOLOGY

A. Principle of haptic feedback

There are four kinds of mechanoreceptors distributed under the surface of human skin, responding to different stimulations such as vibration, shear stress, texture and pressure[12]. The four mechanoreceptors are: Pacinian

978-1-7281-6321-5/19//$31.00 ©2019 IEEE

corpuscles, Meissner's corpuscles, Merkel's discs, and Ruffini endings. Based on their different responses, they can be roughly divided into two categories: fast adaptive receptor and slow adaptive receptor. Among them, Pacinian corpuscles and Meissner's corpuscles are fast-adapting and are only sensitive to active variation such as vibration. Merkel's discs and Ruffini endings are slow-adapted, mainly responding to skin depression caused by stable, static stress. More detailed information of the four receptors is shown in Table I.

TABLE I
CHARACTERISTICS OF FOUR MECHANORECEPTORS[12]

Receptors	*Type (Depth)*	*Adapting Speed*	*Receptive Field*	*Frequency*	*Sensing Property*
Merkel's discs	I	Slow	Small	5-15	Pressure, Texture
Ruffini endings	II	Slow	Large	15-400	Stretch
Meissner's corpuscles	I	Fast	Small	20-50	Stroke, Fluttering
Pacinian corpuscles	II	Fast	Large	60-400	Vibration

Where Type I and type II indicate the distributing position of the receptor under the skin surface layer. Type I receptors are distributed in shallow area, and their receptive field are relatively small. Conversely, type II receptors are distributed in more deep area with larger receptive field.

The haptic feedback based on the ultrasound phased array utilizes acoustic radiation pressure, which is a physical phenomenon caused by acoustic waves in the nonlinear fluid medium. The pressure is proportional to the acoustic energy density of the surface of the object, which is

$$P = 2\alpha \frac{I}{c_0} = \alpha\bar{\varepsilon} = \frac{\alpha p_e^{\,2}}{\rho_0 c_0^{\,2}} \tag{1}$$

Where α is a constant coefficient determined by the medium and the object, I is the sound intensity, c_0 is the speed of sound in the medium, $\bar{\varepsilon}$ is the average sound energy density, p_e is the effective value sound pressure, and ρ_0 is the medium density. Since the energy of the ultrasound is relatively small, even if it is superimposed in an array form, the total acoustic radiation pressure is still insufficient to stimulate slow type receptors that are sensitive to static forces. Whereas Pacinian corpuscles and Meissner's corpuscles, which are sensitive to dynamic changes such as vibration, require much less skin indentation caused by external force[12]. Therefore, the strategy of using the ultrasound phased array for haptic feedback is to control the ultrasound energy distribution to produce sufficient acoustic radiation pressure on the surface of human skin, thus causing certain depth of indentation(14μm for Meissner's corpuscles and 1μm for Pacinian corpuscles). Finally, the ultrasound signal is modulated to a suitable frequency to stimulate two fast-adapting receptors.

B. Modeling of ultrasound arrays

In order to control the energy distribution of the acoustic field, the acoustic radiation pressure of ultrasound array is firstly modeled and analyzed. For an ultrasound transducer shown in Fig. 1(a), it can be modeled as a circular piston model as Fig. 1(b).

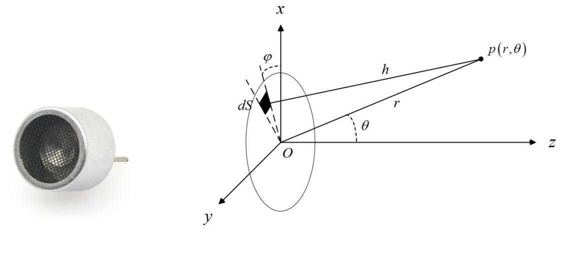

(a) Transducer (b) Model
Fig.1 Ultrasound transducer and circular piston model

By Helmholtz-Huygens formula, also known as the Rayleigh formula, the radiation of the radiating surface is the integration of innumerable point sources, and the sound pressure of the circular piston radiating acoustic field is derived as

$$p(r,\theta,t) = j\frac{\rho_0 \omega u_0 a^2}{2r} \cdot \frac{2J_1(ka\sin\theta)}{ka\sin\theta} \cdot e^{j(\omega t - kr)} \tag{2}$$

Where a is the radius of the circular piston, $k = \omega / c_0$ is the angular wave number, u_0 is the amplitude of the velocity of the particle at the sound source, r and θ are the distance from the point in the sound field space to the center of the sound source and the angle between source-point line and vertical axis. $J_1(*)$ is the first-order Bessel function.

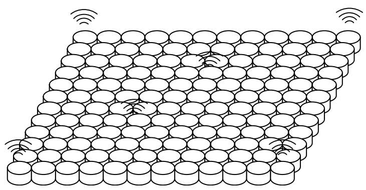

Fig.2 Ultrasound transducer array

For a 12×12 ultrasound array formed as shown in Fig. 2, the sound pressure of the total acoustic field is a linear superposition of the sound field of each single transducer.

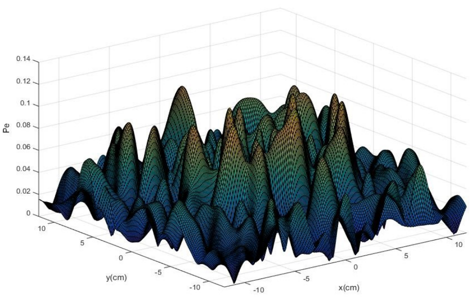

Fig.3 Effective sound pressure under random phase control

In the case of random phase control, the effective sound pressure distribution on the 20cm plane directly above the array is shown in Fig. 3. It can be seen that under random phase control, the sound pressure distribution is messy, which means that the energy cannot be concentrated and the requirements of the haptic feedback cannot be met.

III. ALGORITHM AND OPTIMIZATION

A. *Single focal point*

By flexible control of the phases, variable acoustic field such as sound beam deflection and sound beam focusing as shown in Fig.4 can be formed. For single-point haptic feedback, the method of generating beam focusing is utilized to converge the acoustic field energy to a point.

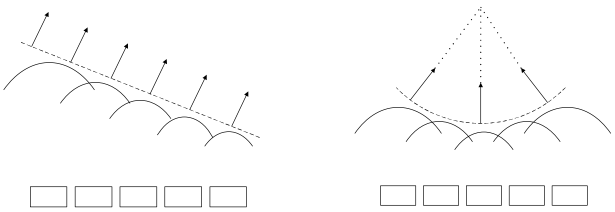

(a) Sound beam deflection (b) Sound beam focusing

Fig.4 Sound beam deflection and beam focusing

For the ultrasound transducer array shown in Fig. 2, a coordinate system as shown in Fig. 5 is established.

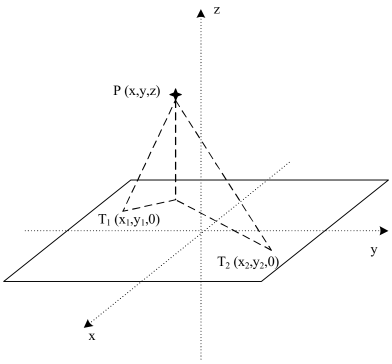

Fig.5 Phase controlled focusing

Then, according to the spatial relationship between the desired focal point and each element, the time required for each transducer in the array to reach the focal point is obtained as,

$$\Delta t_i = \frac{\sqrt{(x-x_i)^2+(y-y_i)^2+z^2}}{c_0} \tag{3}$$

Where (x, y, z) is the coordinate of the focal point and $(x_i, y_i, 0)$ is the coordinate of each transducer. According to the arrival time of each transducer, the corresponding time delay is then obtained, so that the ultrasound waves emitted by each transducer can reach the focal point in the same time.

By setting the desired tactile points at different positions, as shown in Fig. 6(a) and Fig. 6(b), with the yellow cross mark (both on the 20cm plane above the array), the corresponding phase of each transducer are calculated and then represented by different color, as shown in Fig. 6(c) and Fig. 6(d). The effective sound pressure distribution of the total acoustic field for single point focusing are then obtained by applying corresponding phase control, as shown in Fig. 6(e) and Fig. 6(f). It is clear that ultrasound energy is successfully focalized at the desired focal point and noises distributed in other area are very weak.

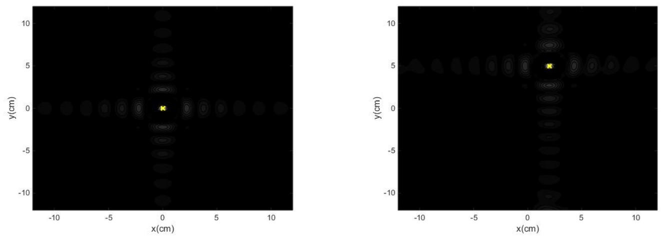

(a) Desired focal point A (b) Desired focal point B

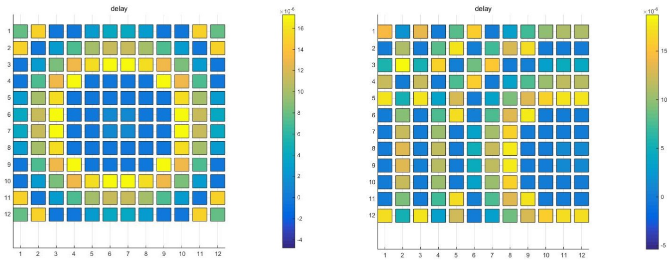

(c) Phase distribution φ_A (d) Phase distribution φ_B

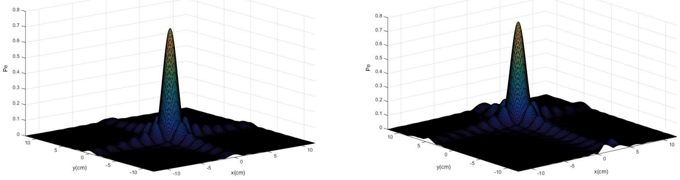

(e) Effective sound pressure P_A (f) Effective sound pressure P_B

Fig. 6 Simulation of single point focusing

B. *Multiple focal point*

In order to generate simultaneous multi-point feedback, a simple approach is to switch between two or more different single-point focused acoustic fields at a high frequency, so that users can feel there are multiple points at the same time. However, switching with such high frequency has higher hardware requirements, and it will inevitably bring about energy loss during each switching. Moreover, unsmooth transitions may even result in the creation of undesired tactile points. Therefore, the goal of this section is to construct a acoustic field with simultaneous multi-point energy focusing. Therefore, it is necessary to analyze the relationship between the phase of the array transducer and the sound pressure of the acoustic field, so as to inversely solve the required phase control by setting the desired sound pressure distribution.

For phase control, we add a phase delay variable in (2) and ignoring the e^{jwt} term since it doesn't affect the effective sound pressure, the amplitude of the sound pressure under the control of a single transducer *delay* is,

$$p(r,\theta)=\left(j\frac{\rho_0\omega a^2}{2r}\cdot\frac{2J_1(ka\sin\theta)}{ka\sin\theta}\cdot e^{j(-kr)}\right)\cdot\left(u_0 e^{j\omega(-delay)}\right) \tag{4}$$

$$p = h\cdot u \tag{5}$$

Where h denotes the forward computation from sound source to space points, and u contains both the amplitude and phase information of the transducer.

Assuming that there are M desired focal points and the number of array elements is N, then the relationship between N sound sources and M focal points is,

$$\begin{pmatrix} h_{11} & \cdots & h_{1N} \\ \vdots & \ddots & \vdots \\ h_{M1} & \cdots & h_{MN} \end{pmatrix} \times \begin{pmatrix} u_1 \\ \vdots \\ u_N \end{pmatrix} = \begin{pmatrix} P_1 \\ \vdots \\ P_M \end{pmatrix} \tag{6}$$

$$Hu = P \tag{7}$$

Where H is an M by N matrix and h_{ij} represents the forward calculation relationship between the i-th focal point and the j-th sound source. Here u is an N by 1 vector containing all sound source information. In most cases, the number of desired focal points is less than the number of transducers in the array, that is, M is less than N. In this case, the number of unknowns is more than the number of equations so that there are countless solutions. A special one is the solution that minimizes the u norm, which is called the minimum norm solution. The problem of solving this minimum norm solution is equivalent to an optimization problem with constraints,

$$\begin{aligned} &\min && \|u\|_2 \\ &\text{subject to} && Hu = P \end{aligned} \tag{8}$$

For this optimization problem, the right inverse is used to get its solution directly,

$$u = H^{*T}\left(HH^{*T}\right)^{-1} P \tag{9}$$

Where H is usually row full rank, so HH^{*T} is reversible.

By setting multiple desired tactile points, we can construct an acoustic field with multi-point focusing, as shown in Fig. 7.

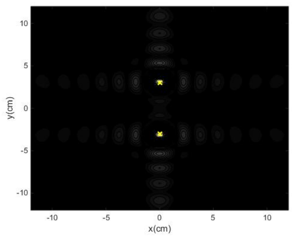

(a) Desired focal points set A

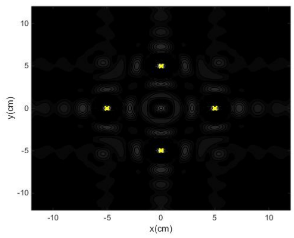

(b) Desired focal points set B

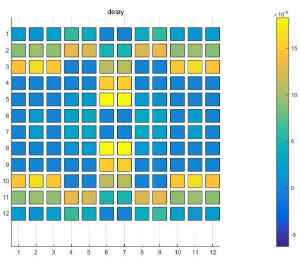

(c) Phase distribution φ_A

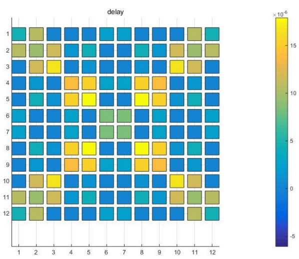

(d) Phase distribution φ_B

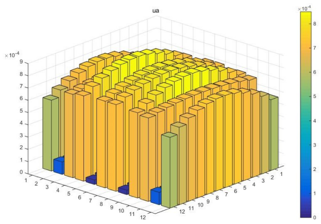

(e) Amplitude distribution U_A

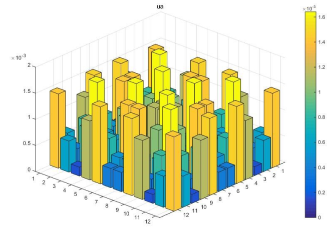

(f) Amplitude distribution U_B

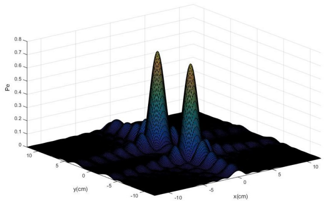

(g) Effective sound pressure P_A

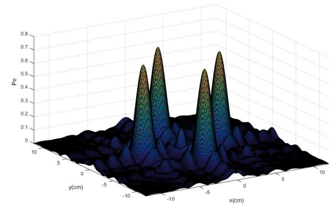

(h) Effective sound pressure P_B

Fig. 7 Simulation of multi-point focusing

Since the variables are not constrained during the solution for multi-point focusing, the amplitudes of transducer array obtained under most cases are not at the same level, as shown in Fig. 7(e) and Fig. 7(f). Obviously, this reduces the output power of the ultrasound array, and it requires more on hardware and software for accurate amplitude control. Therefore, it is necessary to further optimize amplitude and the goal is to make amplitude of each transducer to be as close as possible.

C. *Weighted iterative optimization of amplitude*

In this paper, an iterative weighted optimization algorithm is taken to optimize the amplitude. Here we introduce a weight matrix W in equation (2.26),

$$u_w = WH^{*T}\left(HWH^{*T}\right)^{-1} P \tag{10}$$

Where W is a real positive definite matrix and is optimized by the following iterative method shown in Table II.

TABLE II
WEIGHTED ITERATIVE OPTIMIZATION ALGORITHM

Step 0: Initialize $W = I$

Step 1: $u_w = WH^{*T}\left(HWH^{*T}\right)^{-1} P$

$$\eta = \frac{\sum_{i=1}^{N} |u_i|^2}{NU_{\max}^2} \times 100\%$$

If η meets requirement: jump to Step3; Otherwise: $H^{*T} = WH^{*T}$

Step 2: Update W: $W(m,n) = \begin{cases} \dfrac{1}{u_{wn}}, & \text{for } m = n; \\ 0, & \text{otherwise;} \end{cases}$

Step 3: $u := u_w$

The process of amplitude optimization for a five-point focusing problem is shown in Fig. 8. The amplitude before optimization is shown in Fig. 8(a), and amplitude after 1, 3 and 7 iterations of weighting optimization are shown in Fig. 8(b), Fig. 8(c) and Fig. 8(d) respectively. It's clear that the amplitude of each transducer become very close after only several iterations.

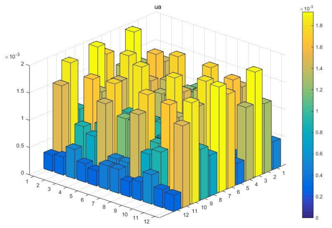

(a) Amplitude before optimization

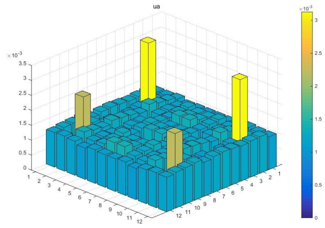

(b) Amplitude after 1 iteration

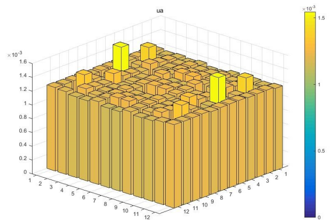

(c) Amplitude after 3 iteration

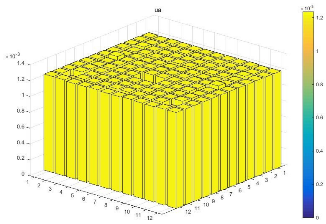

(d) Amplitude after 7 iteration

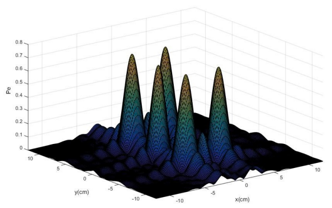

(e) Effective sound pressure before optimization

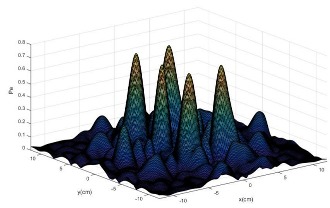

(f) Effective sound pressure after optimization

Fig. 8 Iterative optimization of amplitude

Finally, the effective sound pressure distribution before optimization is shown in Fig. 8(e), and the effective sound pressure distribution based on the optimized amplitude and phase is shown in Fig. 8(f). Although obviously the noise are also amplified and enhanced, their highest value is still at a low level, which means it has little influence on the final haptic feedback.

IV. Conclusion

In this paper, the mechanism of haptic feedback based on ultrasound phased array are discussed, including both the characteristics of four kinds of mechanoreceptors and the focusing of ultrasound. Mathematical model of ultrasound array is established for simulation of its acoustic field. Based on the pseudo inverse method, acoustic fields with simultaneous multi-point focusing are successfully constructed. Further, we optimize the amplitude of the solution for multi-point focusing to improve power efficiency. In the future, visual representation, sound interaction and haptic feedback by ultrasound can be combined together to explore many attracting applications in VR, public intelligent service area and so on.

Acknowledgment

This work was supported by the following funds: 1) National Natural Science Foundation of China (U1713206), 2) Basic Re-search Plan of Shenzhen (JCYJ20170413112645981, JCYJ20150928162432701), and 3) Shenzhen Technology In-novation Program (JCYJ20170811160003571).

References

[1] Ma Z, Edge D, Findlater L, Tan H Z. Haptic keyclick feedback improves typing speed and reduces typing errors on a flat keyboard[C]. World Haptics Conference. IEEE, 2015:220-227.

[2] Massie T H. The PHANTOM Haptic Interface: A Device for Probing Virtual Objects[C]. Proceedings the ASME Winter Meeting, Symposium on Haptic Interfaces for Virtual Environment and Teleoperator Systems. 1994:295-301.

[3] Choi I, Hawkes E W, Christensen D L, Ploch C J, Follmer S. Wolverine: A wearable haptic interface for grasping in virtual reality[C]. IEEE/RSJ International Conference on Intelligent Robots and Systems. IEEE, 2016:986-993.

[4] Suzuki Y, Kobayashi M. Air jet driven force feedback in virtual reality[J]. IEEE Computer Graphics & Applications, 2005, 25(1):44.

[5] Gupta S, Dan M, Patel S N, Tan D. AirWave: Non-Contact Haptic Feedback Using Air Vortex Rings[C]. ACM International Joint Conference on Pervasive and Ubiquitous Computing. ACM, 2013:419-428.

[6] Sodhi R, Poupyrev I, Glisson M, Israr A. AIREAL:interactive tactile experiences in free air[J]. ACM Transactions on Graphics, 2013, 32(4):1-10.

[7] Weiss M, Wacharamanotham C, Voelker S, Borchers B. FingerFlux:near-surface haptic feedback on tabletops[C]. ACM Symposium on User Interface Software and Technology, Santa Barbara, Ca, Usa, October. DBLP, 2011:615-620.

[8] Iwamoto T, Tatezono M, Shinoda H. Non-contact Method for Producing Tactile Sensation Using Airborne Ultrasound[C]. International Conference on Haptics: Perception, Devices and Scenarios. Springer-Verlag, 2008:504-513.

[9] Monnai Y, Hasegawa K, Fujiwara M, Yoshino K, Inoue S, Shinoda H. HaptoMime:mid-air haptic interaction with a floating virtual screen[C]. Proceedings of the 27th annual ACM symposium on User interface software and technology. ACM, 2014:663-667.

[10] Carter T, Seah S A, Long B, Drinkwater B. UltraHaptics:multi-point mid-air haptic feedback for touch surfaces[C]. ACM Symposium on User Interface Software and Technology. ACM, 2013:505-514.

[11] Long B, Seah S A, Carter T, Subramanian S. Rendering volumetric haptic shapes in mid-air using ultrasound[J]. Acm Transactions on Graphics, 2014, 33(6):1-10.

[12] Xin X, Sanwei L, Chenye Y, Zhengyu Y. A Review of Smart Materials in Tactile Actuators for Information Delivery[J]. C, 2017, 3(4):38.